Article

DInSAR Time Series of ALOS PALSAR and ENVISAT ASAR Data for Monitoring Hashtgerd Land Subsidence due to Overexploitation of Groundwater

Nazemeh Ashrafianfar, Wolfgang Busch, Clausthal-Zellerfeld, Germany, Maryam Dehghani, Shiraz, Iran, Steffen Knospe, Clausthal-Zellerfeld, Germany & Mahmud Mohammad Rezapour Tabari, Shahrekord, Iran

Summary: Differential SAR Interferometry (DIn-SAR) is able to monitor land deformation at sub-millimetre as an areal measurement. DInSAR time series calculates land deformation on every radar acquisition date from all individual interferograms in relation to the first/arbitrary date. These calculations help to monitor long term (trend) as much as short terms (seasonal) variations of the land deformation. This research endeavours to investigate the feasibility of a time series algorithm by use of no consecutive radar data in a case study. The Hashtgerd area of north-western Iran is subject to land subsidence resulting from the overexploitation of groundwater. The only tool for areal monitoring subsidence in this area was the DInSAR method. SAR data covering the Hashtgerd Plain include ENVISAT ASAR and ALOS PALSAR data. The interferograms were calculated by ENVISAT ASAR and ALOS PALSAR raw data. For this calculation, the two-pass DInSAR method was applied. Time series algorithm was worked out in three main steps by use of calculated differential interferograms containing less decorrelation, atmospheric effects, topographic and unwrapping error and other noise sources. Firstly, residual orbital tilts and linear atmospheric effects were reduced from all interferograms by use of a least-squares plane fitting approach. Secondly, all interferograms were corrected in relation to one reference point. Finally, DInSAR time series was elaborated by a least-squares-based method integrated with a finite difference approximation approach. This algorithm was successful to link separate groups of interferograms by use of a proper weighting factor, and reduced a nonlinear part of atmospheric effects. The results of Hashtgerd time series calculations showed a relatively constant long term variation of subsidence about 14 cm/yr, in spite of seasonal variations of subsidence. The time series results of

Zusammenfassung: *Monitoring von Bodensenkungen durch Grundwasserentnahme in Hashtgerd basierend auf DInSAR-Zeitreihen der Sensoren ALOS-PALSAR und ENVISAT-ASAR.* Die Differentielle SAR-Interferometrie (DInSAR) ist eine flächenhaft arbeitende Messmethode, mit der Bodenbewegungen im Millimeter-Bereich bestimmt werden können. Mit DInSAR-Zeitreihen lassen sich Bodenbewegungen überwachen, wobei zu jedem Datum einer Radarmessung die Line-of-Sight (LOS) Entfernungsänderung in Bezug auf ein gewähltes (beliebiges Referenz-) Datum bestimmt wird. Diese Berechnungen helfen, sowohl langfristige Trends als auch kurzzeitige, z.B. saisonale, Variationen der Bodenbewegung abzuleiten. In diesem Beitrag wird die Anwendbarkeit eines Algorithmus zur Zeitreihenauswertung untersucht, wobei für das Untersuchungsgebiet nur unterbrochene Zeitreihen aufeinanderfolgender Radardaten zur Verfügung standen.

Die Hashtgerd Ebene im Nordwesten des Iran unterliegt Bodensenkungen, die durch ein übermäßiges Abpumpen des Grundwassers hervorgerufen werden. Die einzige anwendbare Messmethode für eine flächenhafte Überwachung der Bodensenkungen in diesem Bereich ist das DInSAR-Verfahren. Für das Untersuchungsgebiet sind SAR-Daten (ENVISAT-ASAR und ALOS-PALSAR) verfügbar. Die Interferogramme wurden aus den Rohdaten mit der GAMMA Software berechnet. Bei dieser Berechnung wurde das two-pass-DInSAR Verfahren und ein SRTM-Höhenmodell verwendet. Der Zeitreihenalgorithmus gliedert sich in drei Hauptschritte, wobei nur Interferogramme mit hoher Kohärenz und deutlichem Bodenbewegungssignal benutzt werden. Im ersten Schritt werden residuale (Orbit-) Trends und großräumige atmosphärische Effekte reduziert, indem in allen Interferogrammen eine mit einer Kleinste Quadrate

ENVISAT ASAR were compared with the ALOS PALSAR time series results and by GPS data. The DInSAR time series results demonstrated the ability of the time series algorithm applied and the accuracy of the optimal weighting factor determined.

Schätzung angepasste Trendebene abgezogen wurde. Zweitens wurden alle Interferogramme in Bezug auf einen identischen Referenzpunkt außerhalb des durch Bodenbewegungen beeinflussten Gebietes reduziert. Im dritten Schritt wurde die eigentliche Berechnung der Zeitreihen mit einer Ausgleichungsrechnung auf der Basis einer Finite-Differenzen-Approximation durchgeführt.

Die Ergebnisse der Zeitreihenberechnungen zeigten eine relativ konstante langfristige Bodensenkung von etwa 14 cm/Jahr sowie deutliche saisonale Schwankungen der Bodenbewegungen. Die Ergebnisse der ENVISAT-ASAR-Daten-Auswertung wurden den Ergebnissen aus ALOS-PALSAR-Daten sowie GPS-Daten gegenübergestellt. Mit dem vorgestellten Algorithmus konnten auch zeitlich getrennte Blöcke von Interferogrammen durch die Verwendung eines geeigneten Gewichtungsfaktors verbunden sowie ein nichtlinearer Störgrößenanteil (Trend) und atmosphärische Effekte reduziert werden. Die Ergebnisse der DInSAR-Zeitreihenberechnungen belegen die Nutzbarkeit des hier vorgestellten Algorithmus und die Adäquatheit des abgeleiteten Gewichtungsfaktors.

1 Introduction

In most big cities in Iran today progressive land subsidence due to the overexploitation of groundwater is creating some unrecoverable geo-environmental hazards (MOTAGH et al. 2008). The Hashtgerd area of north-western Iran is subject to land subsidence resulting from the overexploitation of groundwater. The first statement prohibiting the development of groundwater exploitation by drilling new wells in Hashtgerd was made by Iran's Ministry of Water and Energy in 1986 (formal declaration no. 1323, 3236/250), extended and is currently in force (ARASTEH 2005). Even after the prohibition of groundwater exploitation, progressive land subsidence in Hashtgerd is still damaging buildings, water and soil quality and is the motive for study of the subsidence in Hashtgerd. The only tool for monitoring subsidence in Hashtgerd is Interferometric Synthetic Aperture Radar (InSAR). InSAR uses radar signals with high spatio-temporal resolutions to measure deformation of the earth's surface (MASSONNET & FEIGL 1998).

Land subsidence in Hashtgerd was monitored for the first time by DEHGHANI et al.

(2008) applying InSAR technique and with four ENVISAT ASAR scenes, over part of summer and autumn 2008. The progressive land subsidence of this area was monitored using 21 ENVISAT ASAR scenes between 2003 and 2008 by ASHRAFIANFAR et al. (2009). However, owing to the gap in consecutive radar data, the time series calculations were done for two separate time series of 2003 – 2004 and 2007 – 2008 (ASHRAFIANFAR et al. 2009). Because of the importance of investigation of long term behaviour of subsidence in this area, this research undertakes to substantiate the feasibility of a time series algorithm by use of the existing no consecutive radar data. To this end, the ENVISAT ASAR and ALOS PALSAR data were ordered by ESA and processed by the DInSAR algorithm. Selection and implementation an effective method of time series calculation returns to the quality and quantity of calculated interferograms. Owing to incomplete consecutive radar data and the properties of the spatio-temporal baselines of the existing radar data, time series calculation was done using a least-squares-based method (BERARDINO et al. 2002), integrated with a finite difference approximation

approach (SCHMIDT & BÜRGMANN 2003). This approach and the process of removing residual orbital tilts of interferograms (e.g. FUNNING et al. 2005, HOFFMANN 2003) are termed as LSFD algorithm in this research. The acronym LSFD refers to the DInSAR time series algorithm of this research, which was developed in MATLAB environment. This algorithm is completed by three steps (see section 3.2). The two main steps of those three are as following: A "Least Squares plane fitting" and a "Least-squares inversion approach" integrated with a "Finite Difference Approximation". The LSFD algorithm used a weighted factor in order to connect separate chains of interferograms. The resulting ENVISAT ASAR time series were corroborated by the results of ALOS PALSAR time series and by GPS data available. The DInSAR time series results demonstrated the accuracy of the DInSAR processing, applied time series algorithm and the ability of the optimum weighting factor used in this algorithm. The results of this research were applied to investigate the linear and nonlinear correlation and relationship between land subsidence and groundwater level data as the main indicator of aquifer compaction (ASHRAFIANFAR & BUSCH 2012). Moreover,

these results are usable to develop the linear and nonlinear simulation models of land deformation (ASHRAFIANFAR et al. 2011, 2013, ASHRAFIANFAR 2013).

This paper presents five sections of the research: Section 2 presents the hydro-geological background and existing radar datasets, section 3 discusses the applied algorithms of DInSAR and LSFD, section 4 presents the results of the time series of ENVISAT ASAR and ALOS PALSAR data and compares these results with GPS data, and section 5 presents the conclusions of the research.

2   Background and Datasets

2.1 *Hydro-geological Properties of the Case Study*

The city of Hashtgerd is the capital of Savojbolagh County, Alborz province in Iran. The Hashtgerd region is located to the west of Karaj and northwest of Tehran (Fig. 1). This area of 1282 km^2 is situated between geographical longitudes of 50° 20' and 51° 10' and latitudes of 35° 27' and 36° 07'. Hashtgerd Plain is located in the Kordan-River ba-
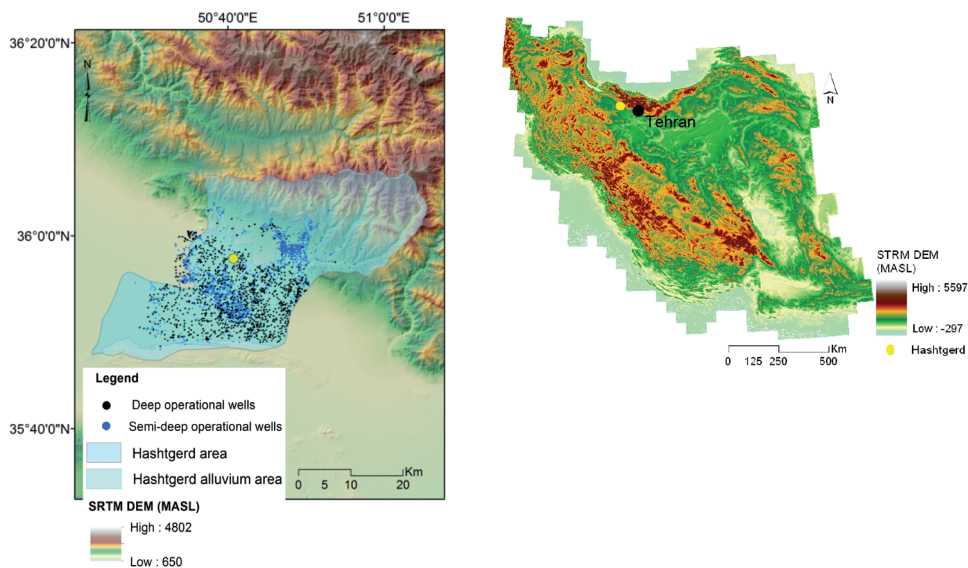

Fig. 1: Situation of the city of Hashtgerd in north-western Iran superimposed on the SRTM digital elevation model of Iran (from DLR) (right). The location of the operational wells over Hashtgerd Plain superimposed on the SRTM DEM (left).

sin of the alluvial area to the south of the Alborz range between Kordan and Abyek. The general slope of the plain is from north-north-east toward the south-west. The study area is mainly located in the part of the Quaternary sediment. With a mild climate and situated near Tehran, the area is consequently highly populated. The growth in population means increased demand for water. The area is mainly farm land and most of the water required for agriculture is provided by 4094 pumping wells. In the Hashtgerd Plain there are 21 piezometric wells with available monthly information for the years between 2003 and 2010. By interpolation of these data the unit hydrograph[1] (MOHAMMAD REZAPOUR TABARI 2009, ZAND & SAHRAEI 2014) of this area was calculated.

This unit hydrograph (Fig. 2) shows a decline of nearly 10 m especially between the

years 1996 and 2001 caused by an excessive pumping out of groundwater (ARASTEH 2005, MOHAMMAD REZAPOUR TABARI 2009) (Fig. 2).

2.2 *Radar Data*

Radar data covering the Hashtgerd Plain include ENVISAT ASAR and ALOS PALSAR data (Tab. 1). These data were ordered from the European Space Agency (ESA). At some locations ENVISAT ASAR data is available every 35 days and ALOS PALSAR data every 46 days. However, there is no such consecutive radar data for the Hashtgerd area. This absence of data aggravates decorrelation arising from vegetation and construction activity as well as provoking additional problems for DInSAR processing.

The ENVISAT ASAR data (45 radar images) include a total of 27 scenes from track 149 between July 2003 and April 2010 and a total of 18 scenes from track 421 between March 2004 and May 2006. All the 45 Level 0 ENVISAT ASAR images, in the descending mode and incidence angle 22.9 degrees, were converted into single look complex (SLC) format using orbital data of the Delft Institute for Earth-Oriented Space Research (by use of GAMMA software). The SLC data were used to calculate interferograms.

ALOS PALSAR data include a total of 14 scenes from track 572 in the ascending mode and incidence angle 38.7 degrees. These scenes cover the time span from June 2007 to November 2010. All the ALOS PALSAR im-

---

[1] The Unit hydrograph of this research was calculated by following steps: 1. Collecting the monthly groundwater level information of the existing piezometric wells, 2. Calculation of the Thiessen area of every piezometric well, 3. Calculation of the mean of groundwater level of all piezome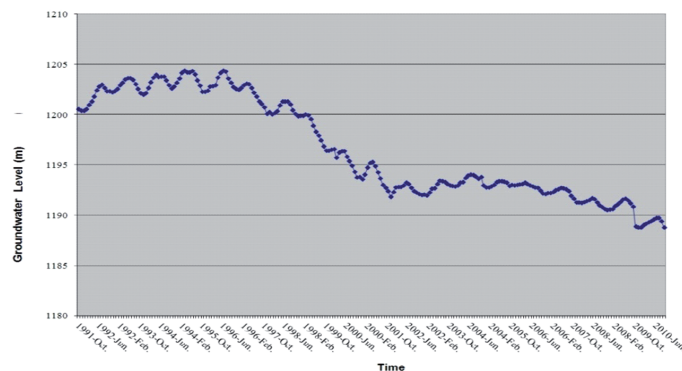tric wells in the area with using of following equation: $h = \left(\sum_{i=1}^{n} A_i \cdot h_i \right) / A$, where, A_i = Area of the Thiessen polygons of piezometer *i* (in *cubic metre*), h_i = Groundwater level of piezometer *i* (in *metre*), and A = Total area of Thiessen polygons of all piezometers (in *cubic metre*), 4. The calculations of step 3 were done for every month and with using of these results of several months during 19 years, the unit hydrograph of Fig. 2 was constructed.

Fig. 2: The unit hydrograph of the Hashtgerd Plain between the years 1991 and 2010 (provided by Groundwater resource management, Ministry of Water and Energy of Iran, 2011).

Tab. 1: Radar acquisition dates and the calculated interferograms as solid lines between two radar dates: ENVISAT ASAR data and the 76 calculated interferograms (left). ALOS PALSAR data and the 18 calculated interferograms (right).

No.	Radar data	Track	Interferograms
1	20030718	149	
2	20030822	149	
3	20030926	149	
4	20031205	149	
5	20040109	149	
6	20040213	149	
7	20040303	421	
8	20040319	421	
9	20040423	421	
10	20040512	421	
11	20040528	149	
12	20040616	421	
13	20040702	149	
14	20040721	421	
15	20040806	149	
16	20040929	421	
17	20040910	149	
18	20041015	149	
19	20041119	149	
20	20041224	149	
21	20050427	421	
22	20050513	149	
23	20050810	421	
24	20050826	149	
25	20050914	421	
26	20051123	421	
27	20060217	149	
28	20060308	421	
29	20060428	149	
30	20071109	149	
31	20080502	149	
32	20080711	149	
33	20080815	149	
34	20080919	149	
35	20081024	149	

No.	RADAR data	Track	Interferograms
1	20070613	527	
2	20080430	527	
3	20080915	527	
4	20080618	527	
5	20090618	527	
6	20090918	527	
7	20100506	527	
8	20101106	527	

ages were converted into single look complex (SLC) format using orbital data of the Delft Institute for Earth-Oriented Space Research (by use of GAMMA software). The SLC data were used to calculate interferograms. A short overview of applied DInSAR procedures is presented in the next section.

3 Methods

3.1 *Differential SAR Interferometry (DInSAR)*

In order to calculate the interferograms, the procedures of the differential SAR interferometry were followed, thus enabling us to attain the differential interferometric phase by combining every two complex SAR images by the following steps (using the GAMMA software):

a. Multilooking was done for the radar images and they were co-registered in order to eliminate some of the noise and to reduce geometrical and atmospheric errors and squint angles.

b. The interferograms were calculated.

c. The SRTM digital elevation model (C band) was used to remove the topographic phase of the interferograms (the last step) and calculation of differential interferograms. Selection of a small perpendicular baseline between every two radar data reduces the topographic error.

d. An adaptive filter, originally by GOLDSTEIN & WERNER (1998), was used on the interferograms to reduce noise contribution in the interferometric phase. In this step, the degree of coherency of interferogram was defined. Higher coherency value shows less decorrelation between two radar images. The interferograms with high coherency value were selected for the next step (unwrapping step).

e. The selected interferograms of the last step were unwrapped by minimum cost flow

(MCF) algorithm. In order to reduce unwrapping error, only a subset of the original interferograms was selected. This subset contained patterns of land deformation in most of the differential interferograms in the Hashtgerd area.

f. The calculated interferograms were projected to the UTM coordinate reference system by geocoding.

Every individual interferogram records the difference phase between two radar acquisition dates, which is in fact an indication of the land deformation between these two dates. The Hashtgerd Plain is mostly a rural area and owing to the changes in the vegetation it produced high decorrelation during the radar observation period. This decorrelation and the existing temporal gap between radar data (Tab. 1) resulted in only a few of the interferograms being usable for time series calculations. A total of 487 interferograms were calculated using the ENVISAR ASAR (SLC) data of both tracks. However, only 76 interferograms used in the time series algorithm were containing less decorrelation, atmospheric effects, unwrapping error, topographic error and spatially constant patterns of land deformation (Tab. 1, left). The temporal difference between the interferograms calculated by EN-VISAT ASAR data is between 35 days and 350 days. A short temporal baseline reduces decorrelation of interferograms. The minimum and maximum perpendicular baselines of the calculated interferograms are 8 m and 860 m, respectively. In addition, a small spatial baseline reduces topographic errors as well as decorrelation of the interferograms. After visual inspection of interferograms, the atmospheric effect of every interferogram was calculated and those interferograms containing less atmospheric effects were selected for time series calculations. This reduces nonlinear atmospheric artifacts on time series calculations.

A total of 28 interferograms were calculated using the ALOS PALSAR (SLC) data. However, considering those parameters of interferograms explained above, only 18 interferograms were used in the time series algorithm (Tab. 1, right). The temporal difference for the calculation of interferograms by ALOS ASAR data is a minimum of 46 days and a maximum of 1242 days. The minimum and maximum perpendicular baselines of the calculated interferograms are 133 m and 4914 m, respectively. In Tab. 1 every interferogram is shown as a line between every two radar acquisition dates. These interferograms were used in the time series calculations of both data types, which is explained in next section.

3.2 *DInSAR Time Series Algorithm*

The calculated interferograms of Tab. 1 were used in the time series algorithm LSFD developed in MATLAB software by the following steps:

a. Removing residual orbital tilts of differential interferograms

A significant component of the atmosphere is linear and acts as an orbital ramp. This part of the atmosphere and the orbital ramp can be reduced by fitting a plane to the points far away from the deformation area (e.g. Funning et al. 2005, Hoffmann 2003, Dehghani et al. 2008). According to Funning et al. (2005), this simple but effective method reduced a part of the linear atmospheric effects of the interferograms.

It should be noted that for reducing the nonlinear atmospheric effects (turbulence effects) those interferograms with high atmospheric effects were not used in the time series calculations (discussed in section 3.1). Also, a weighting factor (W) in step "c" of time series calculations was applied, which reduced a part of the nonlinear atmospheric effects of the time series (Schmidt & Bürgmann 2003, Biggs & Wright 2004).

In this step of the research, the residual orbital tilts of the interferograms were corrected. This step was completed by subtracting a surface fitted to some of the points distributed over parts of the plain which showed no significant subsidence signals (e.g. Funning et al. 2005, Hoffmann 2003, Dehghani et al. 2008, Dehghani 2010). For this aim, a least-squares plane fitting was performed. It is supposed that a plane is definable as (1).

$$ax + by + c = z \tag{1}$$

We considered that every plane is at least constructed using three points. These three points should not be located along one line, or in an area affected by atmospheric or phase unwrapping errors. The least-squares solution for the calculation of residual orbital tilts in the selected points far-off from the deformation area is expressed as (2).

$$z = In \cdot Flt \tag{2}$$

Where at the selected points: z is the calculated differential phase by every interferogram ($INT = 1,\dots, k$); In is the index matrix of the least-squares solution including indices of the plane (1); and Flt is the residual orbital tilt.

The algebraic solution of (2) is expressed as (3) for calculation of Flt.

$$Flt = (In^T \cdot In)^{-1} (In^T \cdot z) \tag{3}$$

Using (3) we fitted a plain to the selected points far-off from deformation area of every interferogram as (4).

$$Flt_{(i,j,k)} = Flt_{(n_1)} \cdot i + Flt_{(n_2)} \cdot j + Flt_{(n_3)} \tag{4}$$

Where i and j are rows and columns of the raster data of every interferogram, respectively; k is the number of the calculated interferograms; n_1, n_2 and n_3 are the selected points in far-fields from deformation area.

The plane (4) is removed from all interferograms according to (5).

$$INT\_Flt_{(i,j,k)} = z_{(i,j,k)} - Flt_{(i,j,k)} \tag{5}$$

Where $INT\_Flt_{(i,j,k)}$ are the flattened interferograms. Now, all interferograms have the same scale in order to use them in the next
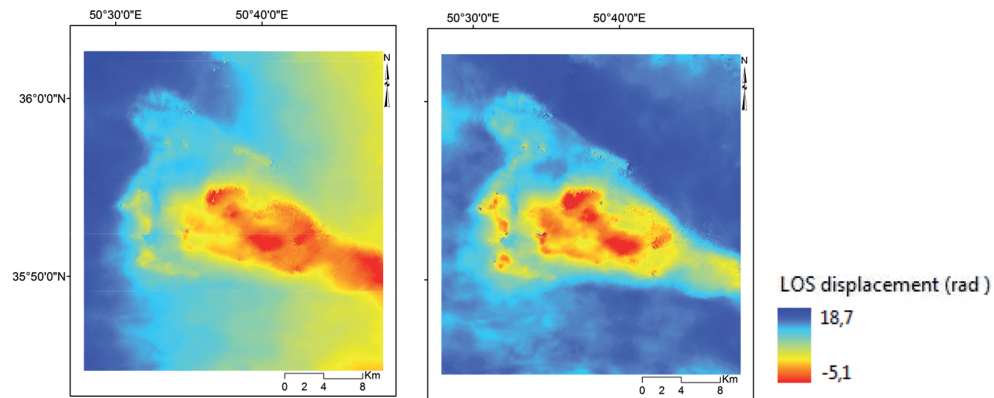

Fig. 3: An Interferogram calculated by ENVISAT ASAR data before (left), and after (right) removal residual orbital tilts. The positive values show subsidence in the line-of-sight (LOS) direction and in radian (15. 8. 2008 – 19. 9. 2008: temporal baseline (Δt) = 35 days, perpendicular baseline ($B_\perp$) = -390.05 m, RMSE = 0.0339 m).

Tab. 2: The maximum and minimum RMSE value of the least-squares plane fitting in order to remove residual the orbital tilts of the interferograms. This value shows the uncertainty of interferograms due to residual orbital tilts and linear atmospheric effects.

Interferogram		Track	Δt (day)	$B_\perp$ (m)	RMSE (m)
ENVISAT ASAR	min. RMSE: 26.9.2003 – 6.8.2004	149	315	166.6	0.0002
	max. RMSE: 13.2.2004 – 2.7.2004	149	140	-443.5	0.0872
	min. RMSE: 10.8.2005 – 8.3.2006	421	210	337.6	0.0027
	max. RMSE: 10.8.2005 – 23.11.2005	421	105	618.1	0.0071
ALOS PALSAR	min. RMSE: 18.9.2009 – 6.11.2010	527	414	1925.7	0.00001
	max. RMSE: 15.9.2008 – 6.5.2010	527	598	3588.7	0.0569

step of the algorithm. An example is given in Fig. 3, which presents an interferogram before and after removal of the residual orbital tilts.

All interferograms of Tab. 1 were processed by this method. The RMSE between the interferograms and the fitted plain in the far-off points is calculated for all interferograms. Tab. 2 presents the minimum and maximum values of the RMSE of the least-squares plane fitting for every radar type. The RMSE shows the uncertainty of interferograms due to residual orbital tilts and linear atmospheric effects.

b. Correction of differential interferograms to zero level

After step a, all interferograms were corrected related to a reference point, located in an area without land deformation. This correction of the interferograms is expressed as (6).

$$INT\_Flt\_ref_{(i,j,k)} = INT\_Flt_{(i,j,k)} - INT\_Flt_{(refY,refX,k)} \quad (6)$$

Where $INT\_Flt\_ref_{(i,j,k)}$ are the corrected interferograms with relation to the reference point ($refY, refX$).

The interferograms resulted by step b are expressed as INT in the following equations of time series algorithm for simplification of writing.

c. Calculation of land deformation in every radar acquisition date by use of the differential interferograms

DInSAR time series monitors land deformation on each radar acquisition date, beginning at the first date and using all calculated individual interferograms. We applied a least-squares-based method (LS) for the InSAR time series calculations. The main principle of the LS method is as follows: If there are at least as many independent interferograms as acquisition dates, and if the chain of interferograms is not broken at any point, it is possible to perform a least-squares inversion method in order to calculate land deformation on each radar acquisition date (BIGGS & WRIGHT 2004).

Accordingly, the relation of the calculated interferograms and deformation on every radar acquisition date $t = [t_1, t_2, t_3, \dots, t_n]$ is ex-

pressed as (7) (BERARDINO et al. 2001, SCHMIDT & BÜRGMANN 2003, BIGGS & WRIGHT 2004):

$$\text{For } \forall (i, j) \rightarrow INT = g \cdot \phi \quad (7)$$

Where $INT = [\varphi_{12}, \varphi_{23}, \dots]$ are the calculated interferograms (the observed land deformation between every two radar acquisition dates); $\phi = [\phi_1, \phi_2, \dots]$ is the unknown phase of land deformation in every radar acquisition date relating to the first date, the deformation in the first date is assumed to be zero ($\phi = 0$); g is the design matrix of LS solution, which links unknown and known values. The rows of the design matrix g is equal to the calculated interferograms (INT) and its columns are as much as the radar acquisition dates minus one (because we assumed the deformation in the first date is equal to zero).

The algebraic solution of (7) is expressed as (8) for the calculation of the land deformation in every radar acquisition date (ϕ).

$$\phi = (g^T \cdot g)^{-1}(g^T \cdot INT) \quad (8)$$

As mentioned before, if $INT \geq \phi$ and the chain of differential interferograms is continuous, the deformation phase in every acquisition date is calculated according to (8). Due to several error sources in the original interferograms (atmospheric, orbital, unwrapping etc.) this calculated time series is not very precise. However, land deformation as a natural phenomenon is considered as a smooth parameter of time (BIGGS & WRIGHT 2004). Therefore, in order to remove the noise partly, other methods are integrated with the LS method described above (BIGGS & WRIGHT 2004). We combined a finite difference approximation with the LS method (SCHMIDT & BÜRGMANN 2003). This integration of methods partially reduces temporal noises of time series as nonlinear atmospheric effects and connects separate groups of differential interferograms of the research. In order to link independent datasets of radar data and mitigate several error types, a finite difference approximation for the second order derivatives of the time series was used as a weighting factor added to (7). The application of this weighting factor (w) presupposes that the velocity of phase of deformation during two sequential time peri-

ods is relatively constant and there are no un-expected significant variations of subsidence (SCHMIDT & BÜRGMANN 2003). To apply this weighting factor (7) is written as (9):

$$\begin{pmatrix} INT \\ 0 \end{pmatrix} = \begin{pmatrix} g \\ w \cdot \dfrac{\partial^2}{\partial t^2} \end{pmatrix} \cdot \phi \qquad (9)$$

Where w is the weighted factor of the LSFD algorithm. The weighting factor (w) was determined optimally by the common method of "trial and error" (e.g. BIGGS & WRIGHT 2004, GAMMA SOFTWARE DOCUMENTATION 2013). An appropriate value of the weighting factor can smooth a noisy time series preserving those nonlinear (seasonal) signals of land deformation (SCHMIDT & BÜRGMANN 2003, BIGGS & WRIGHT 2004). The plot of the root-mean-square error (RMSE) of the LS against various corresponding weighting factors is used in this research (Fig. 4). The RMSE is calculated as (10).

$$RMSE = \sqrt{\frac{1}{k} \cdot \left(\sum_{INT=1}^{k} \hat{R}_{INT} \right)^2} \qquad (10)$$

Where k is the number of the differential interferograms; $\hat{R}_{INT} = (g \cdot \hat{\phi}) - INT$ according to (7), where $\hat{\phi}$ is the estimated phase by the least-squares solution.

We tested several values of W ranging from 0 to 0.15 (Fig. 4) in order to calculate the time series of land deformation. The results of every time series with a specified W were compared to the results of the time series with a very small W (W ~ 0). The subtraction of the time series with a very small W (nearly zero) and a time series with a specified W, e.g. W = 0.02, should show only noise over the whole study area and no significant values of land deformation. This means, only high frequency components of the time series (noises) have been reduced. Finally, the results of the time series with the selected W were compared with the GPS information (see section 4).

Fig. 4 presents the plot of RMSE against different values of weighting factor of the ENVISAT ASAR time series calculations. The overall RMSE by use of weighting factor 0.02 is equal to 1.5 rad (0.0067 m).

The entire time series calculations are repeated using the optimally selected weighting factor for ALOS PALSAR ($w = 0.005$) and ENVISAT ASAR ($w = 0.02$) time series, which eliminates noisy fluctuations from the time series, but preserves the nonlinear (seasonal) signals of deformation. The results of time series calculations are interferometric phases (in radian). These values were converted to deformation along the line-of-sight (LOS) in metre by multiplying $-\lambda / 4\pi$, where λ is the wavelength of the radar data. The LOS displacements were converted to vertical displacement by dividing them by the cosine of incidence angle (θ) of the ENVISAT ASAR ($\theta = 22.9°$) and ALOS PALSAR data ($\theta =$
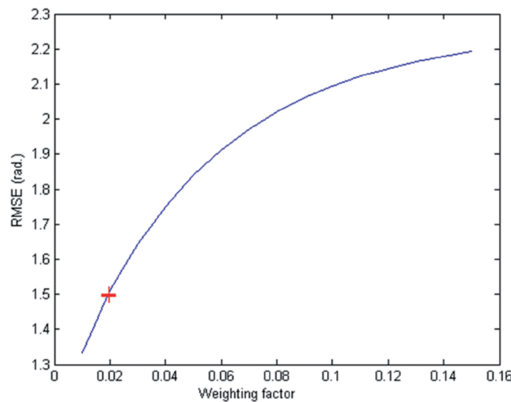

Fig. 4: The optimum weighting factor of the LSFD method used in the ENVISAT ASAR time series calculation at 0.02 rad (0.0067 m) (red cross).

38.7°). The time series results are presented and discussed in the next section.

4   Results and Discussions

The results of ENVISAR ASAR time series showed seasonal variations as uplift and subsidence signals in recharge and discharge periods of Hashtgerd area, respectively. In this area, the discharge drawdown season typically occurs during the period of May to November and the recharge recovery season from December to March (MOHAMMAD REZAPOUR TABARI 2009). The individual results of every discharge period showed that the areas with high subsidence are smaller in the discharge period of 2008 compared with that of 2003. Fig. 5 (left) shows the ENVISAT ASAR annual mean displacement map of the Hashtgerd Plain (between 18.7.2003 and 24.10.2008). The maximum annual rate of subsidence in every year was calculated at 0.142 m.

The time series of ALOS data also showed the seasonal variations of the subsidence. The area with the maximum subsidence has occurred particularly in the centre of the subsidence bowl, and in summer 2010, it seems to extend more toward the east of the area. Fig. 5

(right) represents the ALOS annual displacement map. The maximum annual rate of subsidence was calculated at 0.163 m.

In order to evaluate the results of the InSAR processing and time series calculation, the results of the ENVISAT ASAR and the ALOS PALSAR time series calculation in part of the recharge period of 2008 were compared with each other. Fig. 6 represents the displacement map of the ENVISAT (left: 2.5.2008 – 19.9.2008) and the ALOS time series calculation (right: 30.4.2008 – 15.9.2008). Fig. 7 represents the histogram of the difference between ALOS and ENVISAT displacement maps (mean deviation = ALOS minus ENVISAT). This histogram shows the distribution of the mean deviation of -0.0054 m around zero. This difference of 5 mm stems from several sources, such as different radar data types with various properties, errors contributed in InSAR processing and also the time series calculations. The ALOS PALSAR data with L-band tends to less temporal decorrelation, also less unwrapping errors compared with ENVISAT ASAR data (C-band). The interferograms calculated using ALOS PALSAR data contain smaller numbers of phase jumps and consequently, less unwrapping error. Accordingly, the time series results of ENVI-
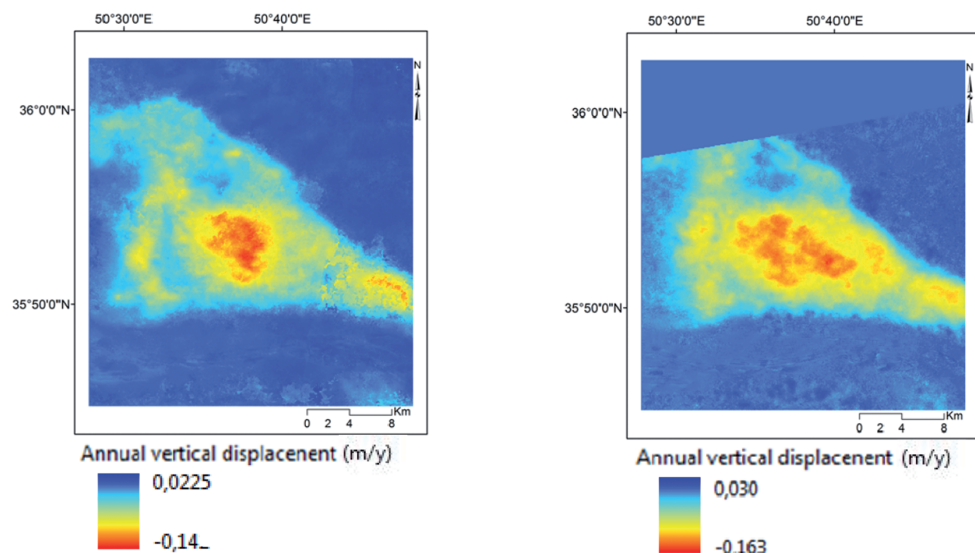

Fig. 5: ENVISAT ASAR annual deformation rate (from 18.7.2003 to 24.10.2008, left), and ALOS PALSAR annual vertical displacement map (from 15.9.2008 to 6.11.2010, right).
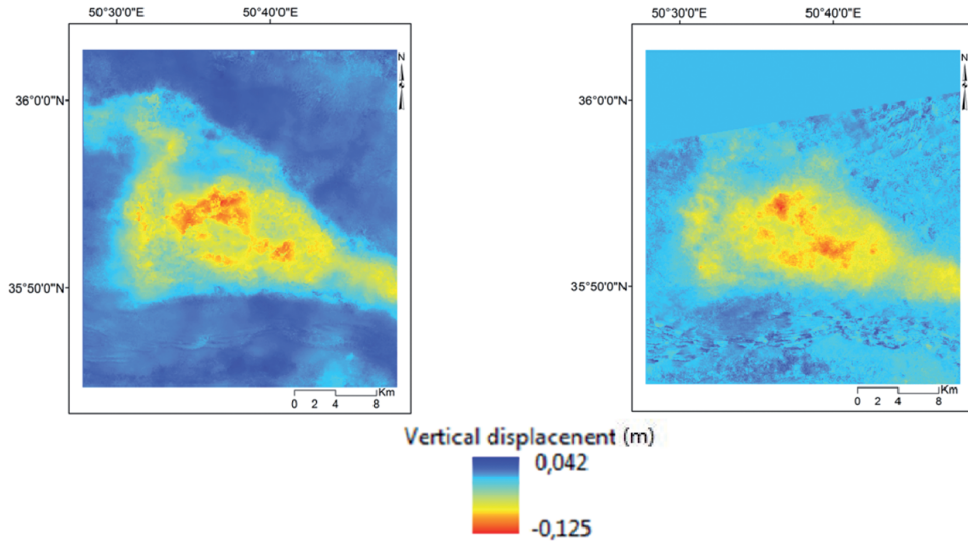
Fig. 6: Comparing the displacement maps of ENVISAT ASAR (left: 2.5.2008 – 19.9.2008) and ALOS PALSAR (right: 30.4.2008 – 15.9.2008).

SAT ASAR data showed an underestimation of vertical displacement in comparison with those of ALOS PALSAR data. The negative value of the mean deviation (-0.0054) is related to this fact.

The GPS information of Hashtgerd was compared with the results of the DInSAR time series of both data types. In the area there is one GPS continuous monitoring station (Najmabad Station) and some GPS periodic monitoring stations. The periodic GPS information was collected by the Geodynamics Group

of the Geological Survey of Iran (GSI) from July to December 2008. The location of periodic GPS stations in the Hashtgerd subsidence area is represented in Fig. 8. The differ-
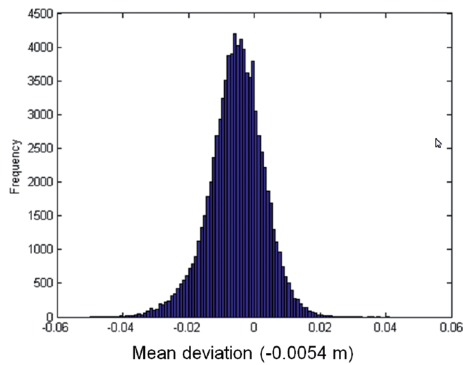
Fig. 7: Histogram of the mean deviation between displacement maps of the ALOS PALSAR and ENVISAT ASAR data (mean deviation = ALOS minus ENVISAT = -0.0054 m).
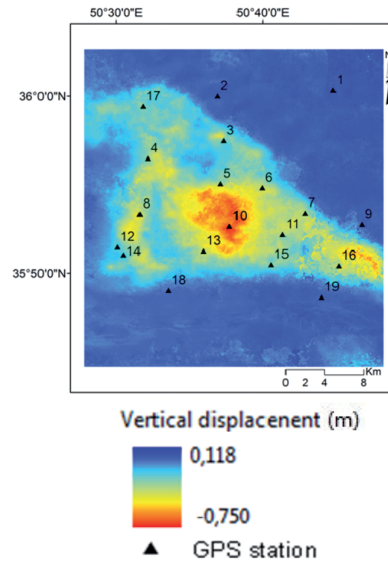

Fig. 8: The location of the GPS periodic monitoring stations in the Hashtgerd subsidence area superimposed on the vertical displacement map of ENVISAT (from 18.7.2003 to 24.10.2008).

ence between discontinues GPS information and time series of ENVISAT and ALOS was calculated at 0.02 m and 0.005 m, respectively (mean deviation = GPS minus ENVISAT/ALOS) (Fig. 9). In accordance with these diagrams, DInSAR measurements show fewer values of the land displacements than those measured by the GPS. This discrepancy can be explained by the differences between the two techniques of subsidence monitoring. The results of the time series of the InSAR-derived subsidence and information of the continuous GPS continuous monitoring station (Fig. 10 left) showed good agreement (Fig. 10 right).

5   Conclusions

The performance of a developed time series algorithm for monitoring long term variation of land subsidence was demonstrated in spite of the incomplete radar data for the case study. This algorithm consists of three steps. Firstly, the residual orbital tilts of interferograms were removed by a least-squares plane fitting approach. Secondly, the interferograms were corrected to zero level. Finally, the land deformation in every radar acquisition date was calculated applying a least-squares inversion approach integrated with a finite difference approximation. The finite difference approxi-
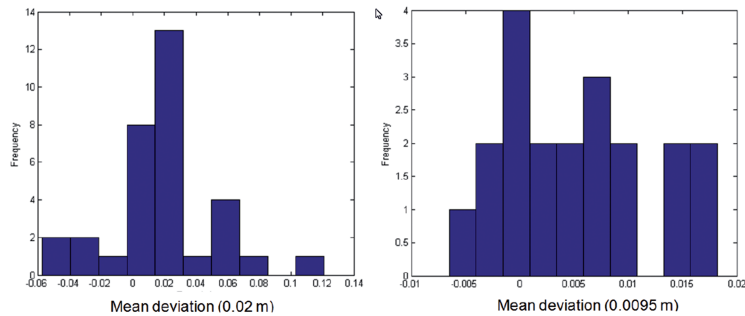

Fig. 9: Histograms of the difference between GPS information and time series calculation results of ENVISAT at 0.0235 m (left) and ALOS PALSAR time series at 0.0095 (right) (mean deviation = GPS-ENVISAT/ALOS).
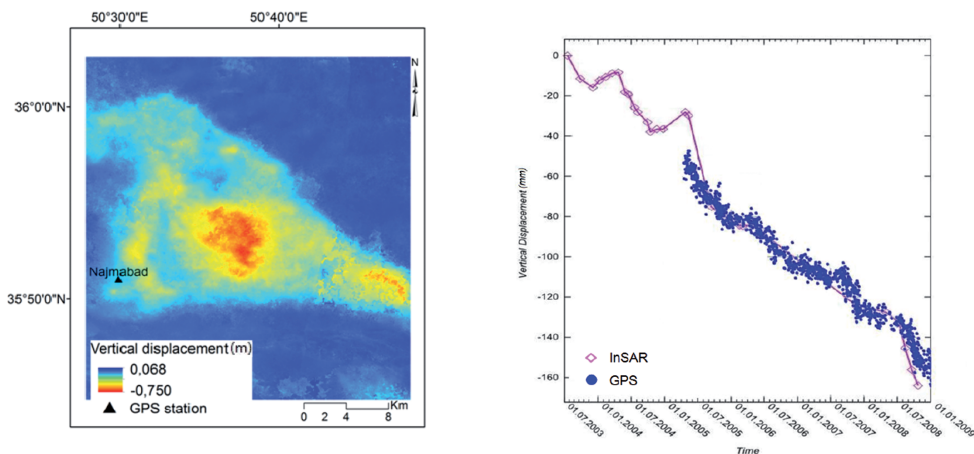

Fig. 10: The location of the GPS continuous monitoring station (Najmabad station) superimposed on the vertical displacement map of ENVISAT ASAR (from 18.7.2003 to 24.10.2008) (left), comparing the information of this station with the ENVISAT ASAR time series (right).

mation for the second order derivatives of the time series was applied as a weighting factor. The weighting factor was determined optimally by the common method of "trial and error". An appropriate value of the weighting factor can smooth a noisy time series, preserving short-term temporal (seasonal) variations of land deformation. The time series results of ENVISAT ASAR with ALOS PALSAR data for a part of the discharge period of the year 2008 and with GPS data showed a good agreement. The results of the Hashtgerd time series calculations showed a relatively constant long term variation of subsidence about 14 cm/yr between years 2003 and 2008.

The DInSAR time series results confirmed the performance of the developed Hashtgerd time series algorithm and demonstrated the ability of the defined weighting factor. These results can be applied for the prediction and assessment of the land deformation in the Hashtgerd area and in order to prevent and/or mitigate subsidence hazards. The long term and seasonal variations of subsidence are both important in groundwater management programmes. Also, the results of the time series are applicable in the linear and nonlinear simulation models of land subsidence and aquifer parameters estimations.

Acknowledgements

References

Arasteh, M., 2005: Report on the continuing prohibition of groundwater exploitation programmes in the Hashtgerd area. – Department of Tehran Water Resources, Ministry of Water and Energy, Iran (Farsi, see below for access).

Ashrafianfar, N., Busch, W., Dehghani, M. & Haghighatmehr, P., 2009: Differential SAR Interferometric technique for land subsidence monitoring due to groundwater over-exploitation in the Hashtgerd. – Fringe 2009, Frascati, Italy.

Ashrafianfar, N., Busch, W., Dehghani, M. & Mohammad Rezapour Tabari, M., 2011: Application of Differential SAR Interferometry technique in a Dynamic Neural Network-based simulation-optimization model for subsidence prediction. – Fringe 2011, 8th International Workshop on "Advances in the Science and Applications of SAR Interferometry", 19–23 September 2011, Frascati, Italy, http://earth.eo.esa.int/workshops/fringe2011/index.php?page=214&type=s (31.7.2014).

Ashrafianfar, N. & Busch, W., 2012: The application of InSAR to monitor pumping induced-land subsidence and its relation with aquifer properties. – GeoHannover 2012, GeoRohstoffe für das 21. Jahrhundert. – Schriftenreihe der Deutschen Gesellschaft für Geowissenschaften (SDGG) **80:** 230.

Ashrafianfar, N., Busch, W., Dehghani, M. & Mohammad Rezapour Tabari, M., 2013: Simulation of Land Subsidence Using InSAR Time Series and Aquifer Parameters in a Neurocomputational Approach. – Living planet symposium, Edinburgh, UK, http://www.livingplanet2013.org/abstracts/850066.htm (31.7.2014).

Ashrafianfar, N., 2013: The Application of Satellite Radar Interferometry in the Development of a Dynamic Neural Model of Land Subsidence Induced by Overexploitation of Groundwater. – Dissertation, Institut für Geotechnik und Markscheidewesen der Technischen Universität Clausthal.

Berardino, P., Fornar, G., Lanari, R. & Sansosti, E., 2002: A new algorithm for surface deformation monitoring based on small baseline differential SAR interferograms. – IEEE Transactions on Geoscience and Remote Sensing **40:** 2375–2383.

Biggs, J. & Wright, T., 2004: Creating a time series of ground deformation using InSAR. – Center of observation and modelling of earthquakes and tectonics, unpublished paper, University of Oxford, UK.

DEHGHANI, M., VALADAN ZOEJ, M.J., BOLOURCHI, M.J. & SHEMSHAKI, A. & SAATCHI, S., 2008: Monitoring of Hashtgerd Land Subsidence Induced by Overexploitation of Groundwater Using SAR Interferometry. – XXIst ISPRS Congress, Technical Commission **VIII:** 365–368.

DEHGHANI, M., 2010: Estimation of deformation rate and modelling of land subsidence induced by groundwater exploitation using interferometry. – Dissertation, K.N.Toosi University of Technology, Iran (Farsi, see below for access).

FUNNING, G.J., PARSONS, B., WRIGHT, T.J., JACKSON, J.A. & FIELDING, E.J., 2005: Surface displacements and source parameters of the 2003 Bam (Iran) earthquake from Envisat advanced synthetic aperture radar imagery. – Journal of Geophysical Research **110:** B09406.

GAMMA SOFTWARE DOCUMENTATION, 2013: GAMMA Interferometric Point Target Analysis Software (IPTA), Reference Manual. – GAMMA Remote Sensing Research and Consulting AG, Gümligen, Switzerland.

GOLDSTEIN, R.M. & WERNER, C.L., 1998: Radar Interferogram Filtering for Geophysical Applications. – Geophysical Research Letters **25** (21): 4035–4038.

HOFFMANN, J., 2003: The application of satellite radar interferometry to the study of land subsidence over developed aquifer systems. – Dissertation, 211 p., Department of Geophysics, Stanford University, CA, USA.

MASSONNET, D. & FEIGL, K.L., 1998: Radar interferometry and its application to changes in the Earth's surface. – Reviews of Geophysics **36** (4): 441–500.

MOTAGH, M., WALTER, T.R., SHARIFI, M.A., FIELDING, E., SCHENK, A., ANDERSSOHN, J. & ZSCHAU, J., 2008: Land subsidence in Iran caused by widespread water reservoir overexploitation. – Geophysical Research Letters **35** (16): L16403.

MOHAMMAD REZAPOUR TABARI, M., 2009: The first step in the Karaj water resources preservation project, Hashtgerd area. – A long-term programme, Reyab Consulting Engineers of Iran (Farsi, see below for access).

SCHMIDT, D.A. & BÜRGMANN, R., 2003: Time-dependent land uplift and subsidence in the Santa Clara Valley, California, from a large interferometric, synthetic aperture radar dataset. – Journal of Geophysical Research **108:** 8534–8543.

ZAND, F. & SAHRAEI, A., 2014: Examining Issues of Groundwater Resources Exploitation in Malayer plain, Iran. – International Journal of Scientific Research in Knowledge **2** (3): 124–133, ISSN: 2322-4541.

For access to the articles in Farsi please contact Mrs. NAZEMEH ASHRAFIANFAR at: nazemeh.ashrafianfar@tu-clausthal.de

Addresses of the Authors:

Dr.-Ing. NAZEMEH ASHRAFIANFAR, Prof. Dr.-Ing. WOLFGANG BUSCH & Dr. rer. nat STEFFEN KNOSPE, Institute of Geotechnical Engineering and Mine Surveying, Clausthal University of Technology, Erzstraße 18, D-38678 Clausthal-Zellerfeld, Tel.: +49-5323-72-2666, Fax: +49-5323-72-2492, e-mail: {nazemeh.ashrafianfar}{wolfgang.busch}{steffen.knospe}@tu-clausthal.de

Dr. MARYAM DEHGHANI, Assistant Professor, Dep. of Civil and Environmental Engineering, School of Engineering, Shiraz University, Zand St., Shiraz, Iran, Tel.: +98-711-6133162, Fax: +98-711-6473161, e-mail: dehghani_rsgsi@yahoo.com

Dr. MAHMOUD MOHAMMAD REZAPOUR TABARI, Assistant Professor, Institute of Geotechnical Engineering, Shahrekord University, Km 2 Saman Road, Post code: 115, Shahrekord, Iran. , Tel.: +98-381-4424401-6, e-mail: mrtabari@eng.sku.ac.ir